ORIGINAL RESEARCH COMMUNICATION

A Curcumin Derivative That Inhibits Vinyl Carbamate-Induced Lung Carcinogenesis *via* Activation of the Nrf2 Protective Response

Tao Shen,[1,2,*] Tao Jiang,[1,*] Min Long,[3] Jun Chen,[4] Dong-Mei Ren,[2] Pak Kin Wong,[5] Eli Chapman,[1] Bo Zhou,[6] and Donna D. Zhang[1,7]

Abstract

Aims: Lung cancer has a high worldwide morbidity and mortality. The employment of chemopreventive agents is effective to reduce lung cancer. Nuclear factor erythroid 2-related factor 2 (Nrf2) mitigates insults from both exogenous and endogenous sources and thus has been verified as a target for chemoprevention. Curcumin has long been recognized as a chemopreventive agent, but poor bioavailability and weak Nrf2 induction have prohibited clinical application. Thus, we have developed new curcumin derivatives and tested their Nrf2 induction. *Results:* Based on curcumin, we synthesized curcumin analogs with five carbon linkages and established a structure–activity relationship for Nrf2 induction. Among these derivatives, bis[2-hydroxybenzylidene]acetone (BHBA) was one of the most potent Nrf2 inducers with minimal toxicity and improved pharmacological properties and was thus selected for further investigation. BHBA activated the Nrf2 pathway in the canonical Keap1-Cys151-dependent manner. Furthermore, BHBA was able to protect human lung epithelial cells against sodium arsenite [As(III)]-induced cytotoxicity. More importantly, in an *in vivo* vinyl carbamate-induced lung cancer model in A/J mice, preadministration of BHBA significantly reduced lung adenocarcinoma, while curcumin failed to show any effects even at high doses. *Innovation:* The curcumin derivative, BHBA, is a potent inducer of Nrf2. It was demonstrated to protect against As(III) toxicity in lung epithelial cells in an Nrf2-dependent manner. Furthermore, compared with curcumin, BHBA displayed improved chemopreventive activities in a carcinogen-induced lung cancer model. *Conclusion:* Taken together, our results demonstrate that BHBA, a curcumin analog with improved Nrf2-activating and chemopreventive activities both *in vitro* and *in vivo*, could be developed into a chemoprotective pharmacological agent. *Antioxid. Redox Signal.* 23, 651–664.

Introduction

LUNG CANCER IS the most commonly diagnosed cancer and is the leading cause of cancer-related deaths worldwide. It has long been recognized that employing chemicals (chemopreventive agents) to enhance our body's ability to detoxify or remove carcinogens is an effective ap-proach to reduce cancer incidence (33, 38). So far, many enzymes, receptors, and signaling pathways have been identified to be potential molecular targets for chemoprevention (29). Among them, activating the nuclear factor erythroid 2-related factor 2 (Nrf2)-dependent defensive response is a proven means of developing cancer chemopreventive agents (21, 22, 50). Nrf2 is a transcription factor that

[1]Department of Pharmacology and Toxicology, College of Pharmacy, University of Arizona, Tucson, Arizona.
[2]Key Laboratory of Chemical Biology (MOE), School of Pharmaceutical Sciences, Shandong University, Jinan, People's Republic of China.
[3]Department of Endocrinology, Xinqiao Hospital, Third Military Medical University, Chongqing, People's Republic of China.
[4]State Key Laboratory of Virology and Modern Virology Research Center, College of Life Sciences, Wuhan University, Wuhan, People's Republic of China.
[5]Department of Aerospace and Mechanical Engineering, University of Arizona, Tucson, Arizona.
[6]State Key Laboratory of Applied Organic Chemistry, Lanzhou University, Lanzhou, People's Republic of China.
[7]Arizona Cancer Center, University of Arizona, Tucson, Arizona.
*These authors contributed equally.

Innovation

Bis[2-hydroxybenzylidene]acetone (BHBA) is a novel nuclear factor erythroid 2-related factor 2 (Nrf2) inducer derived from a lead molecule, curcumin. BHBA was found to potently induce the Nrf2 pathway at nontoxic levels. Furthermore, we demonstrated for the first time that BHBA activated the Nrf2 pathway in the canonical Keap1-Cys151-dependent manner. BHBA was also shown to protect normal human lung epithelial Beas-2B cells against sodium arsenite [As(III)]-induced cytotoxicity. Most importantly, in an *in vivo* vinyl carbamate-induced lung cancer model in A/J mice, preadministration of BHBA significantly attenuated the development of lung adenocarcinoma. Therefore, BHBA is a novel lead toward the development of a chemopreventive agent.

mounts cytoprotective responses against both exogenous and endogenous insults. Under normal conditions, Nrf2 is maintained at a low level through Keap1-mediated ubiquitylation and subsequent 26S proteasome-mediated degradation. However, when cells are exposed to electrophiles or oxidants, Nrf2 is stabilized, Nrf2 levels rise, and free Nrf2 translocates into the nucleus, binds to the antioxidant response element (ARE) located in the promoter region of cytoprotective genes, and upregulates their transcription (21).

The Nrf2 target genes encode proteins with diverse cellular functions and can be divided into three major groups: (i) intracellular redox-balancing proteins, such as glutamate-cysteine ligase (both subunits GCLC and GCLM) and heme oxygenase-1 (HO-1) that maintain the cellular redox capacity and eliminate reactive oxygen species (ROS); (ii) phase II detoxifying enzymes, including NAD(P)H: quinone oxido-reductase 1 (NQO1) and glutathione *S*-transferase (GST), which increase solubility and promote excretion of carcinogenic chemicals; and (iii) transporters, for example, multi-drug resistance-associated proteins that facilitate the removal of carcinogens (21).

The essential role of Nrf2 in chemoprevention has been well documented. For instance, compared with Nrf2 wild-type littermates, Nrf2-null mice had higher incidences of bladder, gastric, intestinal, and skin tumors after mice were exposed to the chemical carcinogens, N-nitrosobutyl(4-hydroxybutyl)amine (19), benzo(a)pyrene (34), azoxymethane, and dextran sodium sulfate (26) or 7,12-dimethylbenz(a)anthracene (49). Therefore, identification and development of chemopreventive compounds that activate the Nrf2-mediated cellular defense system have recently become major research foci of medicinal chemists.

Many compounds have been identified as Nrf2 activators. Several of these compounds are being tested in clinical trials (21, 30). Curcumin, a yellow-pigmented compound from turmeric (*Curcuma longa*), is a principal component of curry (Fig. 1A). *In vivo* and *in vitro* studies have demonstrated that curcumin has various bioactivities and potential medicinal applications, including anticancer, anti-inflammatory, antioxidant, immunomodulatory, and neuroprotective properties (6, 16, 17, 23, 39, 43). Moreover, the chemopreventive potential of curcumin was demonstrated when it was shown to induce phase II detoxifying and antioxidant enzymes, including GST, NQO1, and HO-1 (2, 13, 20). Although several studies suggest that curcumin activates these ARE-driven

transcripts by stimulating the upstream kinase pathways (32, 44), a growing body of evidence indicates that curcumin induces the Nrf2-mediated cellular defense system by modifying Keap1 (2, 12, 13, 36).

Although the chemopreventive effects of curcumin have been demonstrated in cell culture systems and animal models, clinical studies indicate that curcumin has very limited therapeutic potential because of its poor bioavailability (1). Oral ingestion of curcumin results in low plasma and tissue concentration due to poor absorption, quick metabolism, and rapid systemic elimination (1). Given these limitations, we sought to optimize bioavailability and Nrf2 induction potency while mitigating toxic effects through medicinal chemistry. In the present study, we synthesized a collection of curcumin analogs and performed a structure–activity relationship (SAR) analysis for Nrf2 induction. From these studies, the hydroxy-substituted curcumin derivative, bis[2-hydroxybenzylidene]acetone (BHBA), was chosen to be further evaluated for its chemopreventive activity. Our results demonstrate that BHBA is a canonical Nrf2 inducer that conferred Nrf2-dependent protection against As(III)-induced cell toxicity in a lung epithelial cell line *in vitro* and significantly suppressed tumor formation in a carcinogen-induced lung cancer model *in vivo*.

Results

Curcumin weakly activates Nrf2

Using a previously reported cell line where the ARE-luciferase reporter gene was stably incorporated into MBA-MB 231 cells (11), we tested the ability of curcumin (see Fig. 1A for the structure) to induce Nrf2 transcriptional activity. As shown in Figure 1B, curcumin weakly enhanced luciferase activity in the dose range tested ($1.25–80\,\mu M$; toxicity was observed at a dose of $25\,\mu M$ and above). Compared with sulforaphane (SFN) (2.8-fold at $2.5\,\mu M$), *tert*-butylhydroquinone (tBHQ) (3.0-fold at $25\,\mu M$), or cinnamaldehyde (CA) (2.5-fold at $10\,\mu M$), curcumin is a weak Nrf2 inducer with a maximum of 1.5-fold induction. Similarly, the protein levels of Nrf2 and its downstream genes, NQO1 and GCLM, were enhanced by curcumin, but to a lesser extent than observed by SFN ($2.5\,\mu M$) (Fig. 1C). We also measured mRNA levels of Nrf2 and its downstream genes using quantitative real-time reverse transcriptase–polymerase chain reaction (qRT-PCR) (Fig. 1D). Consistent with the previously defined mechanism of SFN, stabilization of Nrf2 at the protein level, curcumin had no effect on Nrf2 mRNA levels, but induced mRNA levels of *NQO1* and *GCLM* in a dose-dependent manner. These data indicate that curcumin is a weak Nrf2 activator.

SAR analysis of curcumin analogs for Nrf2 induction

To obtain curcumin derivatives with improved Nrf2 induction and pharmacological properties, a series of analogs were synthesized. The seven-carbon chain linking the two aromatic rings in curcumin was shortened to give two 5-carbon (C5) curcumin derivative core structures, 1,5-diphenyl-3-pentanone (DPO) and 1,5-diphenyl-(1*E*,4*E*)-pentadien-3-one (DPDEO) (Fig. 2). Results from the ARE-luciferase reporter gene assay with DPO and DPDEO showed that DPO lost its Nrf2 induction activity, while DPDEO had enhanced activity, indicating that the unsaturated carbon bonds are important for
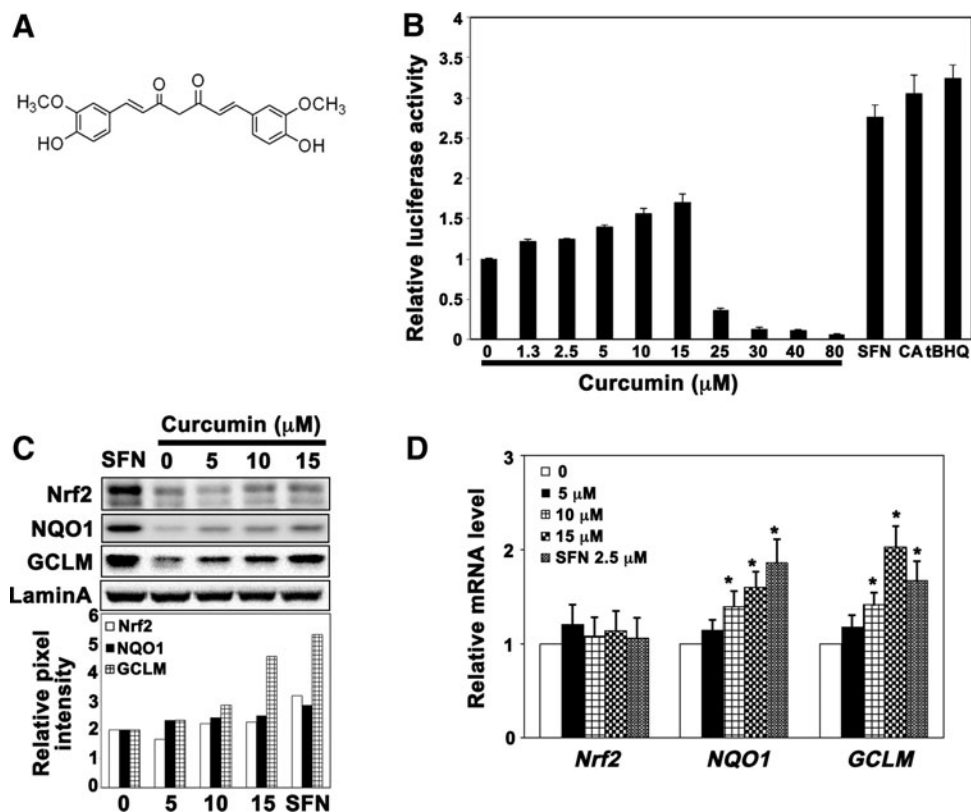
FIG. 1.   Curcumin weakly activated the Nrf2 pathway. (A) Chemical structure of curcumin. **(B)** Curcumin weakly induced ARE-luciferase activity. A stable MDA-MB-231 cell line expressing ARE-luciferase was treated with curcumin (0–80 μM), SFN (2.5 μM), tBHQ (25 μM), or CA (10 μM) for 16 h before luciferase activity was measured. **(C)** Curcumin induced the protein levels of Nrf2, GCLM, and NQO1 slightly. Total cell lysates from MDA-MB-231 cells treated with curcumin (0–15 μM) or SFN (2.5 μM) for 16 h were subjected to immunoblot analysis. **(D)** Curcumin enhanced the mRNA levels of *NQO1* and *GCLM*. mRNA was extracted from MDA-MB-231 cells treated with curcumin (0–15 μM) or SFN (2.5 μM) for 16 h and subjected to quantitative qRT-PCR analysis. Results are expressed as mean $\pm$ SD ($n = 3$), *$p < 0.05$ treated *versus* control. ARE, antioxidant response element; CA, cinnamaldehyde; GCLM, glutamate-cysteine ligase, modifier subunit; NQO1, NAD(P)H: quinone oxidoreductase 1; Nrf2, nuclear factor erythroid 2-related factor 2; qRT-PCR, quantitative real-time reverse transcriptase–polymerase chain reaction; SD, standard deviation; SFN, sulforaphane; tBHQ, *tert*-butylhydroquinone.

Nrf2 induction (Fig. 2). Next, we synthesized three series of curcumin C5 analogs based on the structure of DPDEO: trifluoromethyl substituted (**A** series); hydroxyl substituted (**B** series); and methyl substituted (**C** series). The chemical structures and the ARE-luciferase activities of the synthesized curcumin analogs are shown in Figure 2. The highest dose chosen for each compound was based on 100% survival of cells that were treated with this dose for 16 h. Based on the ability of these compounds to induce ARE-luciferase activity, some interesting conclusions regarding SAR for Nrf2 induction can be drawn: (i) the Michael acceptor groups were essential for inducing ARE-luciferase activity, as seen from the results with DPO and DPDEO; (ii) the positions of substituents on the aromatic rings are associated with their inducing effects, which decreased in the order *ortho*-substitution > *meta*-substitution > *para*-substitution (**A1** > **A2** > **A3**; **A4** > **A5** > **A6**; and similarly for series **B** and **C**; Fig. 2); (iii) disubstituted structures are more potent than monosubstituted structures (**A1** > **A4**; **A2** > **A5**; **A3** > **A6**; and similarly for series **B** and **C**; Fig. 2); and (iv) the Nrf2-inducing effects of substituents decreased with the substitution of trifluoromethyl, methyl, or hydroxyl (**A1** > **C1** > **B1**; **A4** > **C4** > **B4**; **A2** > **C2** > **B2**; Fig. 2). Based on these observations, we concluded that **A1**, **B1**, and

C1 were the curcumin analogs with the strongest Nrf2-inducing activity among the series **A**, **B**, and **C**, respectively.

To further study the mechanism of Nrf2 activation and the chemopreventive potential of these compounds, we selected **B1**, BHBA. The reasons for choosing BHBA were (i) BHBA potently activated ARE-regulated transcription with fivefold increase of ARE-luciferase activity at 4 μM BHBA with low toxicity (Fig. 2, **B1**) and (ii) the hydroxyl-substituted agents were likely to be superior as chemopreventive agents because of enhanced solubility and reduced toxicity relative to **A1** and **C1**. Next, we performed detailed mechanistic studies and protection analyses with BHBA using both *in vitro* and *in vivo* systems.

BHBA activated Nrf2 and its downstream genes in Beas-2B cells

We first evaluated the toxicity of BHBA in Beas-2B cells, a normal lung epithelial cell line, to determine *in vitro* treatment doses. As shown in Figure 3A, when cells were treated with BHBA for 48 h, there was no significant cell toxicity below 4 μM, but 6 μM or higher was toxic. Therefore, 4 μM or less was chosen for subsequent bioassays. The
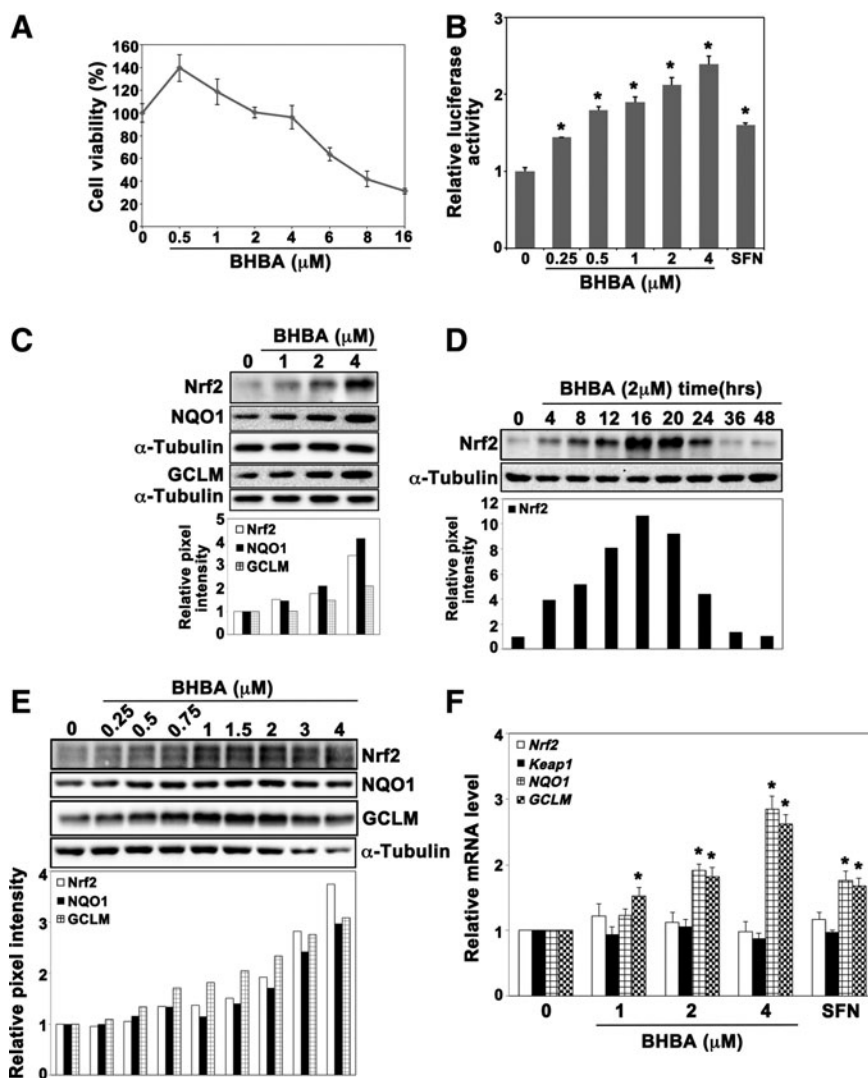
FIG. 2. Structure–activity relationship analysis of curcumin analogs on Nrf2 induction. Curcumin analogs (A, B, and C series) displayed different potencies in Nrf2 induction. The stable MDA-MB-231 cell line expressing ARE-luciferase was used for evaluating Nrf2 induction by curcumin analogs. Cells were treated with the indicated doses of curcumin analogs (μM) for 16 h before luciferase activities were measured. Results are expressed as mean ± SD ($n = 3$).

FIG. 3.   BHBA activated Nrf2 and its downstream genes in human lung epithelial cells. (A) BHBA up to 4 μM did not show cytotoxicity. Beas-2B cells were treated with different doses of BHBA for 48 h; cell viability was measured using the MTT assay. The results are the mean ± SD of three experiments, each in triplicate. **(B)** BHBA induced ARE-luciferase activity in a dose-dependent manner. Beas-2B cells were cotransfected with hNQO1-ARE- and TK-*Renilla* luciferase plasmids for 24 h. The cells were then treated with the indicated doses of BHBA or SFN (2.5 μM) for 16 h. ARE-luciferase and TK-luciferase activities were measured and the ratio of ARE-luciferase/TK-luciferase (the relative luciferase activity) is shown. **(C)** BHBA induced the protein levels of Nrf2, NQO1, and GCLM in a dose-dependent manner. Total cell lysates from Beas-2B cells treated with BHBA (0–4 μM) for 16 h were subjected to immunoblot analysis. **(D)** BHBA induced Nrf2 with a maximum induction at 16 h. Beas-2B cells were treated with BHBA (2 μM) for the indicated duration, and total cell lysates were subjected to immunoblot analysis. **(E)** BHBA induced the protein levels of Nrf2, NQO1, and GCLM in a dose-dependent manner in HBE cells. Total cell lysates from HBE cells treated with BHBA (0–4 μM) for 16 h were subjected to immunoblot analysis. **(F)** BHBA enhanced the mRNA levels of *NQO1* and *GCLM*, but not *Nrf2* and *Keap1*. mRNA was extracted from Beas-2B cells treated with BHBA (0–4 μM) or SFN (2.5 μM) for 16 h and subjected to qRT-PCR analysis. Results are expressed as mean ± SD ($n = 3$), *$p < 0.05$ treated *versus* control. BHBA, bis[2-hydroxybenzylidene]acetone; HBE, human bronchial epithelial cells.

enhanced cell viability observed at low doses of BHBA is most likely due to the enhanced cell proliferation from Nrf2 induction as a similar phenomenon was also observed with other Nrf2 inducers (46). Next, a dual-luciferase reporter gene assay was performed to confirm Nrf2 induction by BHBA in Beas-2B cells. As expected, the ARE-luciferase activity was upregulated by BHBA in a dose-dependent manner (Fig. 3B). Slight induction (1.5-fold) was observed at 0.25 μM and it reached the maximum level (2.5-fold) at 4 μM, indicating that BHBA is more active than the positive control

SFN (1.5-fold at 2.5 μM). Similarly, the protein levels of Nrf2 and its downstream genes, NQO1 and GCLM, increased in a dose-dependent manner after exposure of cells to BHBA for 16 h (Fig. 3C). A time course study of BHBA (2 μM) showed that the Nrf2 protein level increased as early as 4 h, reached the highest level at 16 h, and returned to basal levels by 36 h (Fig. 3D). To confirm that BHBA-mediated Nrf2 induction is not just limited to Beas-2B, another human lung epithelial cell line, human bronchial epithelial cells (HBE), was treated with BHBA as well. Similar to Nrf2 induction observed in
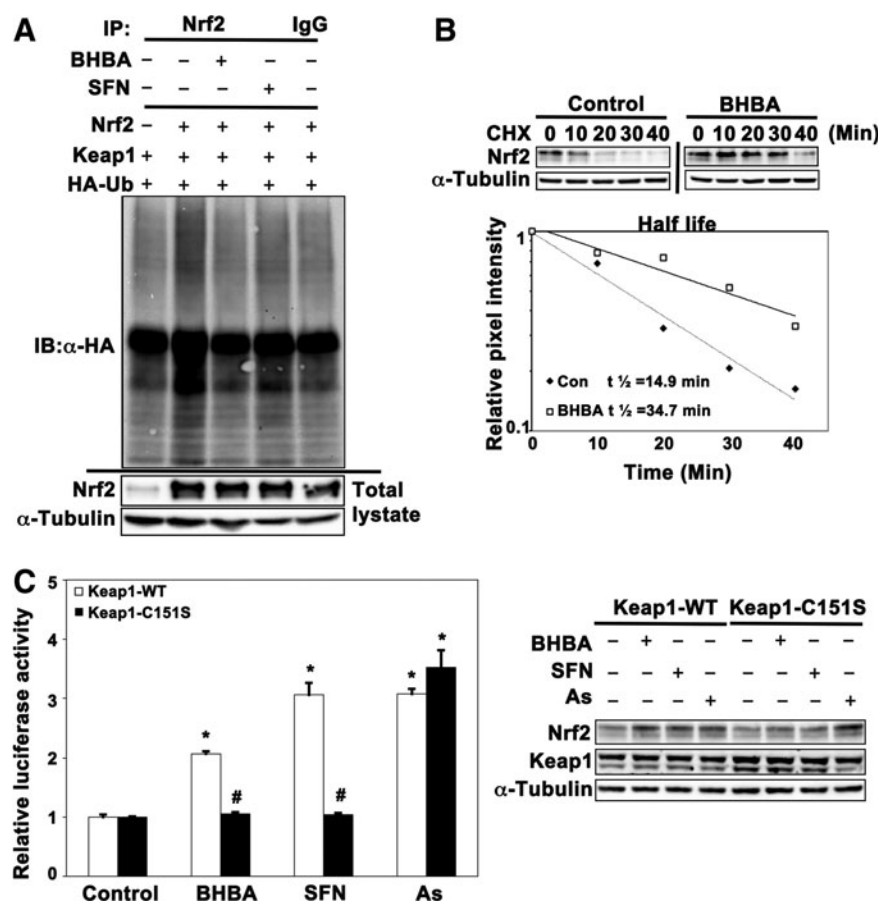
FIG. 4. BHBA blocked Nrf2 ubiquitylation and activated Nrf2 in a Keap1-Cys151-dependent manner. (A) BHBA blocked ubiquitylation of Nrf2. Beas-2B cells, cotransfected with plasmids encoding HA-ubiquitin, Nrf2, and Keap1, were treated with BHBA (4.0 μM) or SFN (2.5 μM) along with MG132 (5 μM) for 4 h. Anti-Nrf2 immunoprecipitates were subjected to immunoblot analysis with anti-HA antibodies for detection of ubiquitylated Nrf2. **(B)** BHBA increased the half-life of Nrf2. Beas-2B cells were left untreated or treated with BHBA (4.0 μM) for 4 h. Cycloheximide (50 μM) was added to block protein synthesis. Cells were lysed at the indicated time point and total cell lysates were subjected to immunoblot analysis using anti-Nrf2 antibodies. The intensity of Nrf2 bands was quantified using Quantity One Software and plotted against the time following cycloheximide treatment. **(C)** BHBA induced the ARE-luciferase activity in a Keap1-Cys151-dependent manner. Beas-2B cells were transfected with Keap1-siRNA that targeted the 5′ untranslated region to knock down endogenous Keap1. Concurrently, Keap1 wild-type (Keap1-WT) or Cys151-mutated Keap1 (Keap1-C151S), together with ARE-firefly luciferase and *Renilla* luciferase, were transfected into these cells, and the cells were exposed to BHBA, SFN, or As(III) for 16 h. ARE-luciferase and TK-luciferase activities were measured and the normalized luciferase activity is shown (*left panel*). Results are expressed as mean ± SD (*n* = 3), *$p < 0.05$ treated *versus* control; #$p < 0.05$ Keap1-WT *versus* Keap1-C151S. An aliquot of cell lysates was subjected to immunoblot analysis (*right panel*). As(III), sodium arsenite; HA, hemagglutinin.

Beas-2B cells, BHBA also induced the Nrf2 signaling pathway in a dose-dependent manner in HBE cells (Fig. 3E). Next, we measured the mRNA levels of Nrf2, Keap1, NQO1, and GCLM in Beas-2B cells treated with BHBA by qRT-PCR. BHBA did not change Nrf2 and Keap1 mRNA levels, as expected, but increased the levels of NQO1 and GCLM (Fig. 3F), suggesting that BHBA induced the Nrf2 pathway through upregulation of Nrf2 at the protein level.

BHBA blocked Nrf2 ubiquitylation and activated Nrf2 in a Keap1-Cys151-dependent manner

To investigate the mechanism of Nrf2 activation by BHBA, we first tested the effect of BHBA in modulating Nrf2 ubiquitylation since Nrf2 stability is regulated through ubiquitin-mediated proteasomal degradation. As shown in Figure 4A,

ubiquitylation analysis indicates that BHBA (4 μM) blocked ubiquitylation of Nrf2 in a manner similar to SFN. Next, we determined the half-life of Nrf2 in the presence or absence of BHBA. The half-life of Nrf2 in untreated cells was 14.9 min and increased to 34.7 min in response to BHBA treatment (4 μM) (Fig. 4B). Taken together, these results indicate that BHBA activated the Nrf2-mediated defensive response by blocking ubiquitylation and thus enhancing Nrf2 stability.

We have previously reported that Cys151 in Keap1 is specifically required for Nrf2 activation by tBHQ, SFN, and tanshinone I (41, 51), whereas the induction of Nrf2 by sodium arsenite [As(III)] and monomethylarsonous acid is independent of Keap1-Cys151 (47). Herein, we investigated whether activation of Nrf2 by BHBA was Cys151 dependent (Fig. 4C). Beas-2B cells were transfected with Keap1-siRNA to remove endogenous KEAP1 and replaced with either Keap1-WT or

Keap1-Cys151S through transfection. The cells were exposed to BHBA, SFN, or As(III) for 16 h before measuring luciferase activities. As expected, all compounds enhanced luciferase activities when the cells were transfected with Keap1-WT. In contrast, induction of luciferase activity by BHBA or SFN was blocked in the cells transfected with Keap1-C151S, indicating that BHBA activated Nrf2 in a Keap1-C151-dependent manner similar to SFN. Consistent with our previous report, As(III) was still able to induce luciferase activity in the cells transfected with Keap1-C151S (47). Next, immunoblot analysis of cell lysates was carried out to confirm the Keap1-C151 dependence. The Nrf2 protein level was upregulated after treatment by all three compounds in the cells ectopically expressing Keap1-WT, whereas only As(III) enhanced the protein level of Nrf2 in the cells transfected with Keap1-C151S (Fig. 4D). These results demonstrate that Cys151 in Keap1 is essential for activation of the Nrf2-mediated defensive response by BHBA.

BHBA protected Beas-2B cells against As(III)-induced cytotoxicity

We next evaluated the protection conferred by BHBA against As(III)-induced cytotoxicity. Beas-2B cells were cotreated with 40 μM As(III) and several doses of BHBA that ranged from 0.25 to 4 μM for 48 h. As shown in Figure 5A, cotreatment with 1.0 μM BHBA exhibited the strongest capacity of countering the As(III)-induced toxicity. It is noted that 2 μM BHBA alone was effective in inducing Nrf2, and treatment of cells with 2 μM BHBA alone showed no toxicity (Fig. 3A, B). However, 1 μM BHBA offered better protection compared with 2 μM BHBA in cells cotreated with BHBA and As(III) as judged by cell viability (Fig. 5A). This is likely due to the added toxicity of both BHBA (off-target toxicity) and As(III). Therefore, 1.0 μM BHBA was chosen for the subsequent *in vitro* protection assays.

Next, as an indication of activation of the Nrf2-mediated protective response in cells, we measured glutathione (GSH) and ROS levels. BHBA significantly enhanced the reduced GSH levels in a dose-dependent manner much more effectively than SFN (Fig. 5B). In addition, treatment with 40 μM As(III) alone increased the intracellular level of ROS significantly, which was reverted by cotreatment with 1.0 μM BHBA, while this dose of BHBA alone had no effect on ROS levels (Fig. 5C). These results indicate that BHBA is able to enhance intracellular redox capacity and inhibit As(III)-induced oxidative stress.
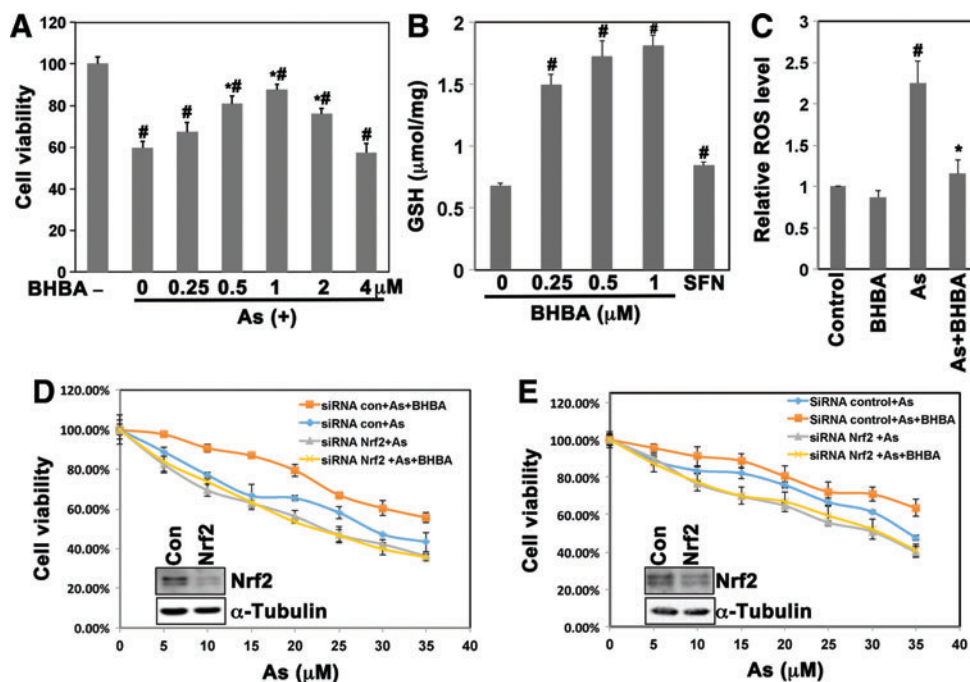

FIG. 5. BHBA protected human lung epithelial cells against As(III)-induced cytotoxicity. (A) Cotreatment with BHBA (1 μM) protected Beas-2B from As(III) toxicity. Beas-2B cells were left untreated or cotreated with As(III) (40 μM) and the indicated dose of BHBA for 48 h. Cell viability was measured using the MTT assay. **(B)** BHBA enhanced the intracellular GSH level in Beas-2B cells. Cells were left untreated (control) or treated with the indicated dose of BHBA or SFN (2.5 μM) for 24 h. The reduced GSH concentration was measured using the QuantiChrom glutathione assay kit. **(C)** BHBA reduced the ROS level. Cells were left untreated or treated with BHBA (1.0 μM), As(III) (40 μM), or BHBA (1.0 μM) and As(III) (40 μM) together for 48 h. The level of ROS was measured using DCF fluorescence with flow cytometry. **(D, E)** BHBA protected Beas-2B or HBE cells against As(III)-induced cytotoxicity in an Nrf2-dependent manner. Beas-2B **(D)** or HBE **(E)** cells were transfected with control-siRNA or Nrf2-siRNA and then treated with the indicated dose of As(III) in the absence or presence of BHBA (1.0 μM) for 48 h. Cell viability was measured by the MTT assay. An aliquot of cell lysates was subjected to immunoblot analysis with anti-Nrf2 antibodies to demonstrate the silenced expression of Nrf2 **(D, E** *insert*). Results are expressed as mean ± SD ($n = 3$), *$p < 0.05$ As(III) *versus* As(III) + BHBA.#$p < 0.05$ As(III) + BHBA *versus* untreated control. GSH, glutathione; ROS, reactive oxygen species. To see this illustration in color, the reader is referred to the web version of this article at www.liebertpub.com/ars.

Finally, we evaluated the protective effect of BHBA against As(III)-induced cytotoxicity and the dependence of this protection on Nrf2 induction in Beas-2B cells (Fig. 5D). Cotreatment with BHBA (1.0 μM) and the indicated doses of As(III) significantly improved the survival of Beas-2B cells compared with As(III) treatment alone (Fig. 5D). However, this BHBA-mediated protection was lost in cells transfected with Nrf2-siRNA (Fig. 5D). Immunoblot analysis supported the effectiveness of Nrf2-siRNA on silencing Nrf2 expression (Fig. 5D, insert). To confirm the protective role of BHBA, the same experiment was performed in HBE cells and similar results were observed (Fig. 5E). These data suggest that BHBA protected lung epithelial cells against As(III)-induced toxicity in an Nrf2-dependent manner.

BHBA inhibited the development of lung adenocarcinoma in A/J mice

A/J mice spontaneously develop lung adenocarcinoma at 2 years of age, but carcinogens, including vinyl carbamate, accelerate the development of tumors, which can usually be detected 16 weeks after vinyl carbamate injections. Therefore, a vinyl carbamate-induced lung cancer model in A/J mice was chosen for evaluation of the chemopreventive potential of BHBA. First, the ability of BHBA to activate Nrf2 in the lungs of A/J mice was measured. Two intraperitoneal injections of BHBA over a 3-day period activated the Nrf2 pathway, as demonstrated by the fact that the protein levels of Nrf2, NQO1, and AKR1C1 increased in the lung tissues (Fig. 6A). For the *in vivo* chemoprevention assay, the mice were injected with BHBA or corn oil seven times over a 2-week period. Vinyl carbamate was injected intraperitoneally (i.p.) twice, at the end of the first and second week after the beginning of BHBA treatment. Mice were sacrificed 16 weeks after the second injection of vinyl carbamate, and the lungs were isolated for further analysis (Fig. 6B). During the course of this study, BHBA was found to have no effect on body weight since the corn oil-treated and the BHBA-treated mice had similar body weights (Fig. 6C). However, a decrease in the weight of the isolated lungs from the BHBA-treated group was observed (Fig. 6D). The lungs were fixed in 10% neutral formalin and visible lung surface tumors were counted. As shown in Figure 6E, the BHBA-treated A/J mice had ∼50% fewer lung surface tumors than the corn oil-treated group (Fig. 6E). More importantly, the administration of curcumin at either low (50 mg/kg) or high (200 mg/kg) dose did not decrease the external lung tumors (Fig. 6E). For microscopic counting of internal tumors, lung tissue sections were hematoxylin and eosin (H&E) stained to reveal separated nodule-like morphology (Fig. 6F, left panel). The number of tumors in one comparable-sized section was counted under a microscope. Consistent with the surface tumor number, BHBA treatment reduced the internal tumor number to nearly 50% compared with the corn oil control (Fig. 6F, right panel). It has been previously reported that vinyl carbamate-induced lung tumors contain a high frequency of K-Ras-activating mutations (31). Therefore, an immunoblot analysis was performed to detect activation of the K-Ras signaling pathway. Although the protein level of K-Ras or total extracellular signal-regulated kinases (ERK) was the same between the two groups, phosphorylated ERK was higher in the control group (Fig. 6G), indicating the suppression of

K-Ras activation by BHBA treatment. Next, activation of the Nrf2 signaling pathway was measured in lung tissues. We did not anticipate an elevated level of Nrf2 in BHBA-treated groups since the lungs were harvested 16 weeks after BHBA injection. In contrast, we thought the untreated tumors might have elevated Nrf2 levels because we recently found that oncogenic activation of K-Ras transcriptionally upregulates Nrf2 (40). As shown in Figure 6I, there were higher levels of Nrf2, AKR1C1, AKR1B10, NQO1, and GCLM in the lung tissues from the corn oil-treated group than in the BHBA-treated group. Immunohistochemistry (IHC) analysis, using several consecutive lung tissue sections, also verified that the higher expression of Nrf2, NQO1, AKR1B10, GCLM, and AKR1C1 was mainly within the tumor regions (Fig. 6H). The expression level of these proteins was similar in normal lung tissues from different groups (data not shown). Taken together, these results demonstrate that BHBA significantly inhibited K-Ras activation and the development of lung adenocarcinoma in vinyl carbamate-induced A/J mice.

Discussion

Curcumin, a polyphenolic compound extracted from the food spice, turmeric, has long been recognized to have antitumor activity. In phase II human clinical trials, oral administration of 4 g of curcumin per day for 30 days reduced aberrant crypt foci (ACF) by 40% in a nonrandomized clinical trial in 44 eligible smokers with ACF (4). However, the use of curcumin as a cancer preventive agent is significantly limited by its poor systemic bioavailability (1). For example, the minimum effective doses are ≥10 μM for cell-based assays and ≥50 mg/kg/day *via* oral administration for rat models (12, 42). Therefore, many researchers have sought to make curcumin analogs with better bioavailability through improved absorption, rapid systemic distribution, and reduced metabolism with the goal of enhancing its antitumor potency.

Curcumin has been shown to exert its anti-inflammatory and anticancer effects through modulation of many important target proteins, including cyclooxygenase-2, NF-κB, and cyclin D1 (4, 14, 15, 27). Recent studies indicate that these activities may also derive from activation of the Nrf2 defense response (2, 12, 24, 42). In the present study, we confirmed that curcumin is a weak Nrf2 activator (Fig. 1). To improve on this activity, we developed a series of curcumin analogs and tested these compounds in a series of *in vitro* and *in vivo* assays. Two curcumin analogs, DPO and DPDEO, with a C5 linker were subjected to an ARE-luciferase assay to evaluate their ability to induce Nrf2 (Fig. 2). Bioactivity results obtained with DPO and DPDEO indicated that the α, β-unsaturated ketone moiety was an essential pharmacophore for Nrf2 induction, supporting the notion that Nrf2 activation by curcumin is most likely through the electrophilic modification of one of the reactive cysteine residues in Keap1. We then performed a detailed SAR analysis of these DPDEO C5 curcumin analogs and selected BHBA as a representative for further mechanistic studies and chemoprevention analyses in cell culture and in a murine lung cancer model.

Our results indicate that BHBA is able to activate the Nrf2 pathway at nontoxic concentrations in Beas-2B cells more potently than curcumin (Figs. 1 and 3), and our findings confirmed the published result that BHBA upregulated
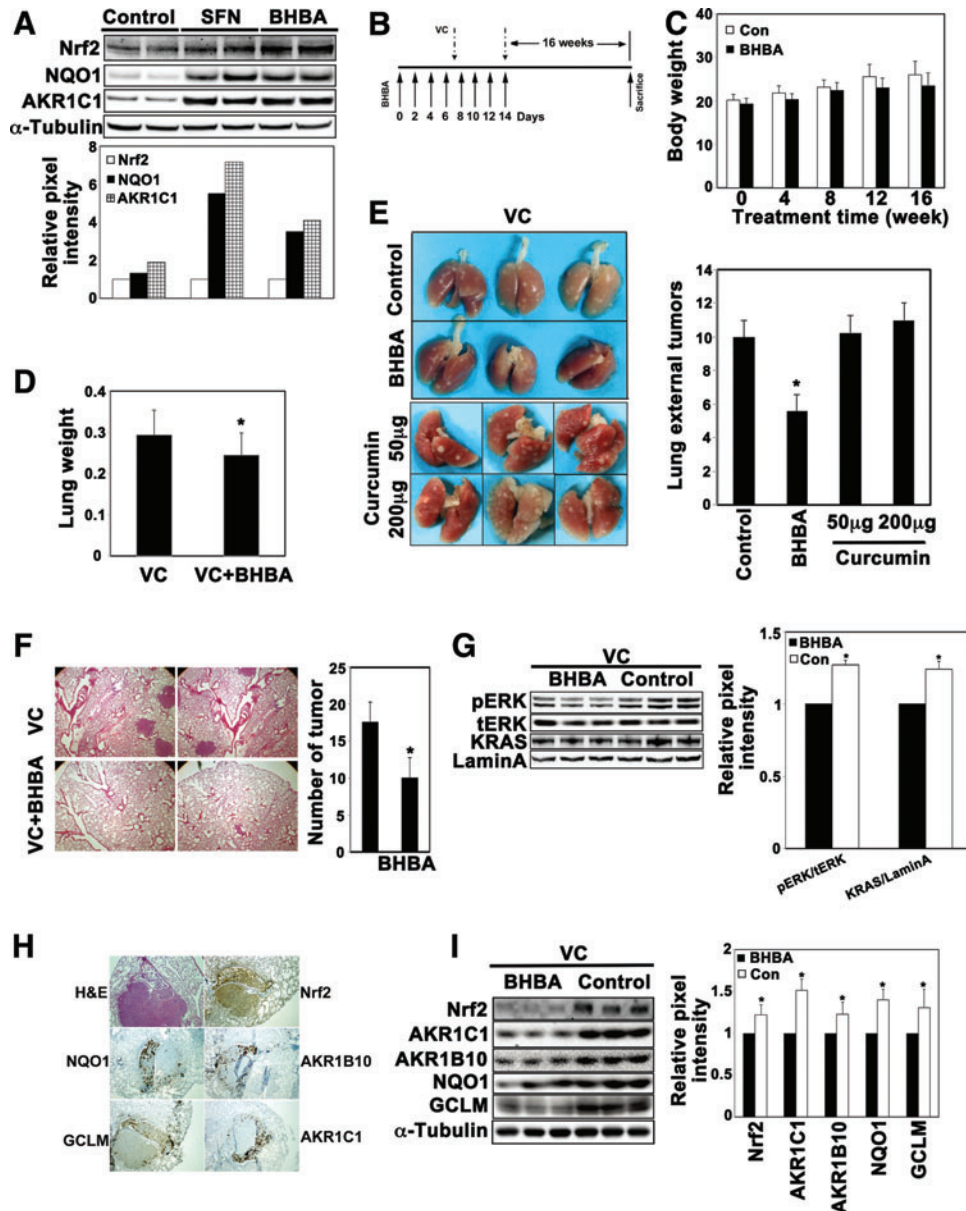
FIG. 6. BHBA inhibited the development of lung adenocarcinoma in A/J mice. **(A)** BHBA activated the Nrf2 signaling pathway in A/J mice. A/J mice received intraperitoneal injections of corn oil, SFN (12.5 mg/kg), or BHBA (20 mg/kg) twice over a 3-day period. Lung tissues were isolated 48 h after the second injection. Tissue lysates were subjected to immunoblot analysis. **(B)** Treatment protocols. Seven-week-old A/J mice were injected i.p. with corn oil (control), BHBA (20 mg/kg), or curcumin (50 or 200 mg/kg) every other day for 2 weeks (*black arrows*). At days 7 and 14, vinyl carbamate (0.32 mg/mouse in 0.1 ml isotonic saline) was injected i.p. to induce tumors (*broken arrows*). Sixteen weeks following the last injection, the mice were sacrificed. **(C)** There was no difference in the body weight between the control and the BHBA-treated group. The body weight of mice was monitored every 4 weeks following the last injection. **(D)** The average weight of the lungs in the BHBA-treated group was less than that in the control group. At the end of 16 weeks, the mice were sacrificed and the lungs were isolated and weighed. *$p < 0.05$ VC *versus* VC + BHBA. **(E)** The number of surface tumors decreased in the BHBA-treated group. Lung tissues were fixed by 10% neutral formalin, and the surface tumors were counted. *$p < 0.05$ BHBA *versus* control. **(F)** BHBA reduced the number of tumors. Fixed lung tissue sections were subjected to H&E staining and the total number of tumors in the largest section was counted under a microscope. **(G)** BHBA suppressed activation of the K-Ras pathway. Tissue lysates were subjected to immunoblotting with K-Ras, total ERK (t-ERK), and phosphorylated ERK (p-ERK) antibodies. *$p < 0.05$ BHBA *versus* control. **(H)** The tumor region expressed higher levels of Nrf2, AKR1C1, AKR1B10, NQO1, or GCLM. Several consecutive fixed lung tissue sections were subjected to IHC analysis with the indicated antibodies. The images were taken under 40× magnification. **(I)** The protein levels of Nrf2 and its target genes were significantly reduced in lung tissues from the BHBA-treated group. Tissue lysates were subjected to immunoblotting with antibodies against Nrf2, AKR1C1, AKR1B10, NQO1, or GCLM. *$p < 0.05$ BHBA *versus* control. ERK, extracellular signal-regulated kinases; H&E, hematoxylin and eosin; IHC, immunohistochemistry; i.p. intraperitoneally. To see this illustration in color, the reader is referred to the web version of this article at www.liebertpub.com/ars

NQO1 enzyme activity in murine leukemia cells in the sub-micromolar range (8–10) (Fig. 3C). In addition, we were able to experimentally confirm that BHBA activated NQO1 enzyme activity through upregulation of Nrf2, which was hypothesized in the previous report, but not verified (8). Similar to SFN and tBHQ, BHBA is a canonical Nrf2 activator that induced Nrf2 in a Keap1-Cys151-dependent manner (Fig. 4). Furthermore, we showed that BHBA blocked ubiquitylation and degradation of Nrf2, thus upregulating the protein level rather than the mRNA level of Nrf2 (Fig. 4). We further investigated if this newly identified canonical Nrf2 inducer is able to be used as a chemopreventive compound to protect cells and tissues against carcinogenic insults using two preclinical lung cancer models: As(III)-induced cytotoxicity in human lung epithelial cells and a carcinogen-induced lung tumor model in A/J mice.

Cigarette smoke has been well documented as the leading cause of lung cancer worldwide, but the widespread environmental contaminant, arsenic, has also been defined as a human carcinogen. Epidemiological studies indicate that arsenic exposure causes many human diseases, including cancer, primarily in the lung, skin, and bladder (3, 5, 28, 45). Hence, we used an As(III)-induced human lung epithelial Beas-2B cell damage model to evaluate the cytoprotective effect of BHBA. Since As(III)-induced depletion of reduced glutathione and thus generation of ROS is directly involved in damage of DNA, lipids, and proteins and plays important roles in cytotoxicity and carcinogenicity of As(III) (7, 37), we measured the levels of glutathione and ROS and found that BHBA treatment enhanced GSH levels and reduced As(III)-induced ROS levels (Fig. 5). Furthermore, cotreatment with BHBA improved cell survival in response to As (III), which was abolished when Nrf2 expression was silenced by Nrf2-siRNA (Fig. 5). Thus, BHBA-mediated protection against As(III) is Nrf2 dependent.

The chemopreventive potential of BHBA was evaluated using a vinyl carbamate-induced lung tumor model in A/J mice. We first established that an intraperitoneal injection of BHBA (20 mg/kg) was able to activate the Nrf2-mediated response in lung tissues (Fig. 6). More significantly, 20 mg/kg BHBA reduced the tumor number to 50%, while curcumin at 50 and 200 mg/kg showed no tumor reduction. To establish a proper chemopreventive protocol, we considered recent findings indicating the dark side of Nrf2 in cancer, that is, cancer-promoting activities of Nrf2 (18, 25, 48). It was revealed that Nrf2 promotes tumor growth when tumors have been initiated (35). To avoid this possibility, in our study, the pretreatment of BHBA only lasted for 2 weeks with seven injections and stopped as soon as the second injection of vinyl carbamate started. The rationale for this protocol is that pretreatment of BHBA for 2 weeks should upregulate Nrf2 target genes, including phase II detoxifying enzymes, redox-balancing proteins, and transporters. Together, these enzymes or proteins are ready to detoxify vinyl carbamate, diminish its ability to transform cells, and thus block the initiation of lung carcinogenesis. Another important observation is that the BHBA-treated group showed lower levels of Nrf2 and its downstream genes at the end of the experiment (Fig. 6). This is because the mice were sacrificed 16 weeks after BHBA injection and BHBA ceased to induce the Nrf2 pathway 2 days after the last injection. Furthermore, our results demonstrated that the K-Ras-Erk pathway was activated

in vinyl carbamate-induced lung tumors (Fig. 6), which is consistent with the previous finding, demonstrating high incidence of K-Ras mutation in vinyl carbamate-induced lung tumors (31), along with our recent finding that oncogenic activation of the K-Ras pathway transcriptionally upregulated Nrf2 through a TPA response element, which then resulted in high expression of Nrf2 and its target genes and promoted tumor progression (40). In this study, BHBA was found to suppress K-Ras activation and tumor initiation, thus reducing the K-Ras-induced transcriptional upregulation of Nrf2 and suppressing expression of Nrf2 target genes (Fig. 6).

In this study, we performed an in-depth SAR analysis of curcumin analogs for their Nrf2-activating potential in an attempt to identify a curcumin derivative with improved activity and bioavailability for chemoprevention. BHBA was the best compound, considering both the potency in Nrf2 induction and the cytotoxic effects, and therefore was selected for detailed characterization. To our knowledge, this is the first study showing BHBA as an Nrf2 inducer that activates the Nrf2 signaling pathway in a canonical Keap1-Cys151-dependent manner. Similar to other canonical Nrf2 inducers, BHBA protects lung epithelial cells against arsenic toxicity. More importantly, BHBA was studied *in vivo* for the first time here. Using A/J mice, we demonstrated the ability of i.p. administered BHBA to induce NRF2 and to protect against lung tumorigenesis. Therefore, BHBA has chemopreventive potential to protect against carcinogenesis *via* activation of the Nrf2-mediated cellular defense system. Based on these promising results, a detailed pharmacokinetic and pharmacodynamic analysis of BHBA is warranted.

Materials and Methods

Chemicals

SFN, tBHQ, CA, and $NaAsO_2$ [As(III)] were purchased from Sigma (St. Louis, MO). Vinyl carbamate (purity >99%) was purchased from Toronto Research Chemicals (North York, ON, Canada). Curcumin analogs were designed and synthesized by our laboratories.

Cell culture

Human breast cancer MDA-MB-231 cells and normal human lung epithelial Beas-2B and HBE cells were purchased from American Type Culture Collection (Manassas, VA). MDA-MB-231 cells were maintained in Eagle's minimal essential medium supplemented with 10% fetal bovine serum, 2 mM HEPES, and 6 ng/ml insulin. Beas-2B cells were cultured in Ham's F-12 medium supplemented with 2.0 mg/ml insulin, 10 μg/ml epidermal growth factor, 2.5 mg/ml transferrin, 0.05 mM dexamethasone, 10 μg/ml cholera toxin, and 6.0 mg/ml endothelial cell growth supplement. All cells were incubated at 37°C in a humidified incubator containing 5% CO_2.

Cell viability assay

Cell viability was determined by the 3-(4,5-dimethylthiazol-2-yl)-2,5-diphenyltetrazolium bromide (MTT) assay. Beas-2B cells (2.0×10^4 cells/well) were seeded in a 96-well plate and treated with the indicated dose of each compound for the indicated time period. After addition of 20 μl MTT (2.0 mg/ml) solution, the cells were incubated at 37°C for 3 h,

and the cell viability was determined by measuring the absorbance at 570 nm on a Synergy 2 plate reader (BioTeK, Winooski, VT).

Luciferase reporter gene assay

A stable ARE-luciferase reporter cell line previously established in our laboratory, MDA-MB-231-ARE-Luc, was used for measurement of Nrf2 induction by curcumin and its analogs (11). The cells were treated with several doses of each compound for 16 h, and the luciferase activity was measured. For the dual-luciferase reporter gene assay, Beas-2B cells were transfected with expression plasmids for both an ARE-firefly luciferase and a TK-*Renilla* luciferase. At 36 h post-transfection, the transfected cells were treated with compounds for an additional 16 h, and then firefly and *Renilla* luciferase activities were measured by the dual-luciferase reporter gene assay system (Promega, Madison, WI). Firefly luciferase activity was normalized to *Renilla* luciferase activity.

Antibodies and immunoblot analysis

The antibodies for Nrf2, Keap1, NQO1, GCLM, lamin A, and α-tubulin were purchased from Santa Cruz Biotechnology (Santa Cruz, CA). Cells were lysed in a sample buffer (50 mM Tris-HCl [pH 6.8], 2% sodium dodecyl sulfate [SDS], 10% glycerol, 100 mM dithiothreitol, 0.1% bromophenol blue). After denaturation and sonication, cell lysates were fractionated by sodium dodecyl sulfate–polyacrylamide gel electrophoresis (SDS-PAGE) and subjected to immunoblot analysis.

Ubiquitylation assay and protein half-life measurement

For the ubiquitylation assay, cells were transfected with expression vectors for hemagglutinin (HA)-ubiquitin, Nrf2, and Keap1. The transfected cells were either left untreated or treated with compounds along with 10 μM MG132 (Sigma) for 4 h. Cells were lysed with a buffer containing 2% SDS, 150 mM NaCl, 10 mM Tris-HCl, and 1 mM DTT. After fivefold dilution of the cell lysates with the buffer lacking SDS, protein A beads (Invitrogen, Carlsbad, CA), anti-Nrf2, and anti-IgG antibodies were added to allow binding overnight at 4°C. Immunoprecipitated proteins were subjected to immunoblot analysis with a ubiquitin antibody. To measure the half-life of Nrf2, cells were either treated or untreated for 4 h. Cycloheximide (10 μM) was added to block protein synthesis. Total cell lysates were collected at desired time points and subjected to immunoblot analysis with anti-Nrf2 antibodies. The relative intensity of the bands was quantified by the ChemiDoc CRS gel documentation system and Quantity One software (Bio-Rad, Hercules, CA). The intensity *versus* time point was plotted on a semilog scale.

Quantitative real-time reverse transcriptase–polymerase chain reaction

Total mRNA was extracted from cells using TRI Reagent (Sigma), and equal amounts of RNA (1 μg) were reverse transcribed to cDNA using the Transcriptor First Strand cDNA Synthesis Kit (Roche, Indianapolis, IN). Primers were synthesized by Sigma and the sequences are as follows:

hNrf2, forward (ACACGGTCCACAGCTCATC) and reverse (TGTCAATCAAATCCATGTCCTG); hKeap1, forward (ACCACAACAGTGTGGAGAGGT) and reverse (CGATCC TTCGTGTCAGCAT); hNQO1, forward (ATGTATGACAAA GGACCCTTCC) and reverse (TCCCTTGCAGAGAGTAC ATGG); hGCLM, forward (GACAAAACACAGTTGGAAC AGC) and reverse (CAGTCAAATCTGGTGGCATC); and hβ-actin, forward (CCAACCGCGAGAAGATGA) and reverse (CCAGAGGCGTACAGGGATAG).

Taqman probes were purchased from the Roche Universal Probe Library: hNrf2 (#70), hKeap1 (#49), hNQO1 (#87), hGCLM (#18), hβ-actin (#64). Duplicate reactions were performed for each sample. The quantitative real-time PCR condition was one cycle of initial denaturation (95°C for 4 min), 45 cycles of amplification (95°C for 10 s and 60°C for 30 s), and a cooling period (40°C for 30 s). The data presented are relative mRNA levels normalized to β-actin, and the value from the untreated group was set as 1.

Glutathione assay and ROS detection

Intracellular reduced glutathione concentration was measured using the QuantiChrom glutathione assay kit from BioAssay Systems (Hayward, CA). Beas-2B cells were treated with the indicated doses of BHBA or SFN (2.5 μM) for 24 h. All procedures were carried out according to the manufacturer's instructions. Samples were run in triplicate for each experiment, and the value from the untreated group was set as 1. The data represent the mean ± standard deviation (SD) of three independent experiments. For ROS analysis, Beas-2B cells were left untreated or pretreated with BHBA (1 μM) for 24 h, then left untreated or treated with As(III) (40 μM) for an additional 24 h. Cells were washed with phosphate-buffered saline (PBS) and the fresh medium containing 2′,7′-dichlorodihydrofluorescein diacetate (10 μg/ml final concentration; Sigma) was added. Cells were incubated for 30 min at 37°C, trypsinized, and resuspended in PBS to ~10^6 cells/ml. Fluorescence was measured by flow cytometry with excitation at 488 nm and emission at 520 nm. The experiments were repeated thrice, with triplicate samples in each experiment, and data are expressed as mean ± SD.

Animal study

Female A/J mice, 7 weeks of age, were obtained from the Jackson Laboratory (Bar Harbor, ME). The mice were acclimatized to laboratory conditions for 1 week before use. First, a pilot experiment was conducted to determine the dose range of BHBA on Nrf2 induction in the lungs of A/J mice. Six mice were randomly divided into three groups ($n=2$), which were injected i.p. with corn oil, SFN (12.5 mg/kg body weight), or BHBA (20 mg/kg body weight) twice over a 3-day period. The lungs were harvested 2 days after the last injection, and lung tissue lysates were subjected to immunoblot analysis with antibodies against Nrf2, AKR1C1, or NQO1. Next, 20 mice were randomly divided into 2 groups ($n=10$) and were injected i.p. with corn oil or BHBA (20 mg/kg body weight) every other day for 2 weeks. At the end of the first and second week, both groups were injected i.p. with vinyl carbamate (0.32 mg/mouse in 0.1 ml isotonic saline). Mice were monitored for body weight every 4 weeks during a period of 16 weeks. At the end of the experiment, the mice were sacrificed and the lungs were isolated and weighed. The

lungs were then fixed in 10% neutral formalin, and the number of tumors on lung surfaces was counted. The fixed lung tissues were paraffin embedded, and tissue sections were subjected to H&E staining and IHC analysis. The number of tumors in a comparable section of the whole lung was counted under a microscope at low power.

Statistical analysis

Results are expressed as mean ± SD. Statistical tests were performed using SPSS 10.0. The ANOVA test with Bonferroni correction was applied to compare the means of three or more groups. Unpaired Student's t-tests were used to compare the means of two groups. $p < 0.05$ was considered to be significant.

Acknowledgments

Author Disclosure Statement

References

1. Anand P, Kunnumakkara AB, Newman RA, and Aggarwal BB. Bioavailability of curcumin: problems and promises. *Mol Pharm* 4: 807–818, 2007.

2. Balogun E, Hoque M, Gong P, Killeen E, Green C, Foresti R, Alam J, and Motterlini R. Curcumin activates the haem oxygenase-1 gene via regulation of Nrf2 and the antioxidant-responsive element. *Biochem J* 371: 887–895, 2003.

3. Byrd DM, Roegner ML, Griffiths JC, Lamm SH, Grumski KS, Wilson R, and Lai S. Carcinogenic risks of inorganic arsenic in perspective. *Int Arch Occup Environ Health* 68: 484–494, 1996.

4. Carroll RE, Benya RV, Turgeon DK, Vareed S, Neuman M, Rodriguez L, Kakarala M, Carpenter PM, McLaren C, Meyskens FL, Jr., and Brenner DE. Phase IIa clinical trial of curcumin for the prevention of colorectal neoplasia. *Cancer Prev Res (Phila)* 4: 354–364, 2011.

5. Chen C, Chen C, Wu M, and Kuo T. Cancer potential in liver, lung, bladder and kidney due to ingested inorganic arsenic in drinking water. *Br J Cancer* 66: 888, 1992.

6. Dhillon N, Aggarwal BB, Newman RA, Wolff RA, Kunnumakkara AB, Abbruzzese JL, Ng CS, Badmaev V, and Kurzrock R. Phase II trial of curcumin in patients with advanced pancreatic cancer. *Clin Cancer Res* 14: 4491–4499, 2008.

7. Ding W, Hudson LG, and Liu KJ. Inorganic arsenic compounds cause oxidative damage to DNA and protein by inducing ROS and RNS generation in human keratinocytes. *Mol Cell Biochem* 279: 105–112, 2005.

8. Dinkova-Kostova AT, Cory AH, Bozak RE, Hicks RJ, and Cory JG. Bis (2-hydroxybenzylidene) acetone, a potent inducer of the phase 2 response, causes apoptosis in mouse leukemia cells through a p53-independent, caspase-mediated pathway. *Cancer Lett* 245: 341–349, 2007.

9. Dinkova-Kostova AT, Holtzclaw WD, Cole RN, Itoh K, Wakabayashi N, Katoh Y, Yamamoto M, and Talalay P. Direct evidence that sulfhydryl groups of Keap1 are the sensors regulating induction of phase 2 enzymes that protect against carcinogens and oxidants. *Proc Natl Acad Sci U S A* 99: 11908–11913, 2002.

10. Dinkova-Kostova AT, Massiah MA, Bozak RE, Hicks RJ, and Talalay P. Potency of Michael reaction acceptors as inducers of enzymes that protect against carcinogenesis depends on their reactivity with sulfhydryl groups. *Proc Natl Acad Sci U S A* 98: 3404–3409, 2001.

11. Du Y, Villeneuve NF, Wang X-J, Sun Z, Chen W, Li J, Lou H, Wong PK, and Zhang DD. Oridonin confers protection against arsenic-induced toxicity through activation of the Nrf2-mediated defensive response. *Environ Health Perspect* 116: 1154, 2008.

12. Farombi EO, Shrotriya S, Na H-K, Kim S-H, and Surh Y-J. Curcumin attenuates dimethylnitrosamine-induced liver injury in rats through Nrf2-mediated induction of heme oxygenase-1. *Food Chem Toxicol* 46: 1279–1287, 2008.

13. Garg R, Gupta S, and Maru GB. Dietary curcumin modulates transcriptional regulators of phase I and phase II enzymes in benzo [a] pyrene-treated mice: mechanism of its anti-initiating action. *Carcinogenesis* 29: 1022–1032, 2008.

14. Goel A, Jhurani S, and Aggarwal BB. Multi-targeted therapy by curcumin: how spicy is it? *Mol Nutr Food Res* 52: 1010–1030, 2008.

15. Gupta SC, Patchva S, and Aggarwal BB. Therapeutic roles of curcumin: lessons learned from clinical trials. *AAPS J* 15: 195–218, 2013.

16. Hamaguchi T, Ono K, and Yamada M. REVIEW: curcumin and Alzheimer's disease. *CNS Neurosci Ther* 16: 285–297, 2010.

17. Hatcher H, Planalp R, Cho J, Torti F, and Torti S. Curcumin: from ancient medicine to current clinical trials. *Cell Mol Life Sci* 65: 1631–1652, 2008.

18. Hayes JD and McMahon M. The double-edged sword of Nrf2: subversion of redox homeostasis during the evolution of cancer. *Mol Cell* 21: 732–734, 2006.

19. Iida K, Itoh K, Kumagai Y, Oyasu R, Hattori K, Kawai K, Shimazui T, Akaza H, and Yamamoto M. Nrf2 is essential for the chemopreventive efficacy of oltipraz against urinary bladder carcinogenesis. *Cancer Res* 64: 6424–6431, 2004.

20. Iqbal M, Sharma SD, Okazaki Y, Fujisawa M, and Okada S. Dietary supplementation of curcumin enhances antioxidant and phase II metabolizing enzymes in ddY male mice: possible role in protection against chemical carcinogenesis and toxicity. *Pharmacol Toxicol* 92: 33–38, 2003.

21. Jaramillo MC and Zhang DD. The emerging role of the Nrf2–Keap1 signaling pathway in cancer. *Genes Dev* 27: 2179–2191, 2013.

22. Jeong W-S, Jun M, and Kong A-NT. Nrf2: a potential molecular target for cancer chemoprevention by natural compounds. *Antioxid Redox Signal* 8: 99–106, 2006.

23. Jurenka JS. Anti-inflammatory properties of curcumin, a major constituent of *Curcuma longa*: a review of preclinical and clinical research. *Altern Med Rev* 14: 141, 2009.

24. Kang ES, Woo IS, Kim HJ, Eun SY, Paek KS, Kim HJ, Chang KC, Lee JH, Lee HT, and Kim J-H. Up-regulation of aldose reductase expression mediated by phosphatidylinositol 3-kinase/Akt and Nrf2 is involved in the protective effect of curcumin against oxidative damage. *Free Radic Biol Med* 43: 535–545, 2007.

25. Kensler TW and Wakabayashi N. Nrf2: friend or foe for chemoprevention? *Carcinogenesis* 31: 90–99, 2010.

26. Khor TO, Huang M-T, Prawan A, Liu Y, Hao X, Yu S, Cheung WKL, Chan JY, Reddy BS, and Yang CS. Increased susceptibility of Nrf2 knockout mice to colitis-

associated colorectal cancer. *Cancer Prev Res (Phila)* 1: 187–191, 2008.

27. Kunnumakkara AB, Diagaradjane P, Anand P, Harikumar KB, Deorukhkar A, Gelovani J, Guha S, Krishnan S, and Aggarwal BB. Curcumin sensitizes human colorectal cancer to capecitabine by modulation of cyclin D1, COX-2, MMP-9, VEGF and CXCR4 expression in an orthotopic mouse model. *Int J Cancer* 125: 2187–2197, 2009.

28. Lau A, Whitman SA, Jaramillo MC, and Zhang DD. Arsenic-mediated activation of the Nrf2-Keap1 antioxidant pathway. *J Biochem Mol Toxicol* 27: 99–105, 2013.

29. Lee KW, Bode AM, and Dong Z. Molecular targets of phytochemicals for cancer prevention. *Nat Rev Cancer* 11: 211–218, 2011.

30. Magesh S, Chen Y, and Hu L. Small molecule modulators of Keap1-Nrf2-ARE pathway as potential preventive and therapeutic agents. *Med Res Rev* 32: 687–726, 2012.

31. Massey TE, Devereux TR, Maronpot RR, Foley JF, and Anderson MW. High frequency of K-ras mutations in spontaneous and vinyl carbamate-induced lung tumors of relatively resistant B6CF1 (C57BL/6J x BALB/cJ) mice. *Carcinogenesis* 16: 1065–1069, 1995.

32. McNally SJ, Harrison EM, Ross JA, Garden OJ, and Wigmore SJ. Curcumin induces heme oxygenase 1 through generation of reactive oxygen species, p38 activation and phosphatase inhibition. *Int J Mol Med* 19: 165–172, 2007.

33. Mehta RG, Murillo G, Naithani R, and Peng X. Cancer chemoprevention by natural products: how far have we come? *Pharm Res* 27: 950–961, 2010.

34. Ramos-Gomez M, Dolan PM, Itoh K, Yamamoto M, and Kensler TW. Interactive effects of nrf2 genotype and oltipraz on benzo [a] pyrene–DNA adducts and tumor yield in mice. *Carcinogenesis* 24: 461–467, 2003.

35. Satoh H, Moriguchi T, Takai J, Ebina M, and Yamamoto M. Nrf2 prevents initiation but accelerates progression through the Kras signaling pathway during lung carcinogenesis. *Cancer Res* 73: 4158–4168, 2013.

36. Shen G, Xu C, Hu R, Jain MR, Gopalkrishnan A, Nair S, Huang M-T, Chan JY, and Kong AN. Modulation of nuclear factor E2-related factor 2–mediated gene expression in mice liver and small intestine by cancer chemopreventive agent curcumin. *Mol Cancer Ther* 5: 39–51, 2006.

37. Shi H, Shi X, and Liu KJ. Oxidative mechanism of arsenic toxicity and carcinogenesis. *Mol Cell Biochem* 255: 67–78, 2004.

38. Sporn MB and Suh N. Chemoprevention: an essential approach to controlling cancer. *Nat Rev Cancer* 2: 537–543, 2002.

39. Srivastava RM, Singh S, Dubey SK, Misra K, and Khar A. Immunomodulatory and therapeutic activity of curcumin. *Int Immunopharmacol* 11: 331–341, 2011.

40. Tao S, Wang S, Moghaddam SJ, Ooi A, Chapman E, Wong PK, and Zhang DD. Oncogenic KRAS confers chemoresistance by upregulating NRF2. *Cancer Res* 74: 7430–7441, 2014.

41. Tao S, Zheng Y, Lau A, Jaramillo MC, Chau BT, Lantz RC, Wong PK, Wondrak GT, and Zhang DD. Tanshinone I activates the Nrf2-dependent antioxidant response and protects against As (III)-induced lung inflammation *in vitro* and *in vivo*. *Antioxid Redox Signal* 19: 1647–1661, 2013.

42. Tapia E, Soto V, Ortiz-Vega KM, Zarco-Márquez G, Molina-Jijón E, Cristóbal-García M, Santamaría J, García-Niño WR, Correa F, and Zazueta C. Curcumin induces Nrf2 nuclear translocation and prevents glomerular hypertension, hyperfiltration, oxidant stress, and the decrease in antioxidant enzymes in 5/6 nephrectomized rats. *Oxid Med Cell Longev* 2012: 269039, 2012. DOI: 10.1155/2012/269039.

43. Taylor RA and Leonard MC. Curcumin for inflammatory bowel disease: a review of human studies. *Altern Med Rev* 16: 152–156, 2011.

44. Thangapazham RL, Sharma A, and Maheshwari RK. Multiple molecular targets in cancer chemoprevention by curcumin. *AAPS J* 8: E443–E449, 2006.

45. Tokar EJ, Benbrahim-Tallaa L, Ward JM, Lunn R, Sams RL, 2nd, and Waalkes MP. Cancer in experimental animals exposed to arsenic and arsenic compounds. *Crit Rev Toxicol* 40: 912–927, 2010.

46. Wang XJ, Sun Z, Chen W, Eblin KE, Gandolfi JA, and Zhang DD. Nrf2 protects human bladder urothelial cells from arsenite and monomethylarsonous acid toxicity. *Toxicol Appl Pharmacol* 225: 206–213, 2007.

47. Wang X-J, Sun Z, Chen W, Li Y, Villeneuve NF, and Zhang DD. Activation of Nrf2 by arsenite and monomethylarsonous acid is independent of Keap1-C151: enhanced Keap1–Cul3 interaction. *Toxicol Appl Pharmacol* 230: 383–389, 2008.

48. Wang X-J, Sun Z, Villeneuve NF, Zhang S, Zhao F, Li Y, Chen W, Yi X, Zheng W, and Wondrak GT. Nrf2 enhances resistance of cancer cells to chemotherapeutic drugs, the dark side of Nrf2. *Carcinogenesis* 29: 1235–1243, 2008.

49. Xu C, Huang M-T, Shen G, Yuan X, Lin W, Khor TO, Conney AH, and Kong A-NT. Inhibition of 7, 12-dimethylbenz (a) anthracene-induced skin tumorigenesis in C57BL/6 mice by sulforaphane is mediated by nuclear factor E2-related factor 2. *Cancer Res* 66: 8293–8296, 2006.

50. Yu X and Kensler T. Nrf2 as a target for cancer chemoprevention. *Mutat Res* 591: 93–102, 2005.

51. Zhang DD and Hannink M. Distinct cysteine residues in Keap1 are required for Keap1-dependent ubiquitination of Nrf2 and for stabilization of Nrf2 by chemopreventive agents and oxidative stress. *Mol Cell Biol* 23: 8137–8151, 2003.

Address correspondence to:
Dr. Donna D. Zhang
Department of Pharmacology and Toxicology
University of Arizona
1703 E. Mabel Street
Tucson, AZ 85721

E-mail: dzhang@pharmacy.arizona.edu

Dr. Bo Zhou
State Key Lab of Applied Organic Chemistry
Lanzhou University
222 Tianshui Street S.
Lanzhou 730000
P.R. China

E-mail: bozhou@lzu.edu.cn

Dr. Eli Chapman
Department of Pharmacology and Toxicology
University of Arizona
1703 E. Mabel Street
Tucson, AZ 85721

E-mail: chapman@pharmacy.arizona.edu

Abbreviations Used

ACF = aberrant crypt foci
ARE = antioxidant response element
As(III) = sodium arsenite
BHBA = bis[2-hydroxybenzylidene]acetone
C5 = 5-carbon
CA = cinnamaldehyde
ERK = extracellular signal-regulated kinases
GCLM = glutamate-cysteine ligase, modifier subunit
GSH = glutathione
GST = glutathione *S*-transferase
HA = hemagglutinin

H&E = hematoxylin and eosin
HBE = human bronchial epithelial cells
HO-1 = heme oxygenase-1
IHC = immunohistochemistry
i.p. = intraperitoneally
NQO1 = NAD(P)H: quinone oxidoreductase 1
Nrf2 = nuclear factor erythroid 2-related factor 2
PBS = phosphate-buffered saline
qRT-PCR = quantitative real-time reverse transcriptase–
            polymerase chain reaction
ROS = reactive oxygen species
SAR = structure–activity relationship
SD = standard deviation
SDS-PAGE = sodium dodecyl sulfate–polyacrylamide
            gel electrophoresis
SFN = sulforaphane
tBHQ = *tert*-butylhydroquinone